Liquid Crystals
Publication details, including instructions for authors and subscription information:
http://www.informaworld.com/smpp/title~content=t713926090

New TGB_A series exhibiting a S_C*$S_A$$S_A$*N* phase sequence

A. Bouchta[ab]; H. T. Nguyen[a]; M. F. Achard[a]; F. Hardouin[a]; C. Destrade[a]; R. J. Twieg[c]; A. Maaroufi[b]; N. Isaert[d]
[a] Centre de Recherche Paul Pascal, Pessac Cedex, France [b] Département de Chimie, Université de Tetouan, Tetouan, Morocco [c] IBM Almaden Research Center, San Jose, California, U.S.A. [d] Laboratoire de Dynamique et Structure des Matériaux Moléculaires, (U.R.A, CNRS No. 801), Université de Lille 1, Villeneuve d'Ascq Cedex, France

To cite this Article Bouchta, A. , Nguyen, H. T. , Achard, M. F. , Hardouin, F. , Destrade, C. , Twieg, R. J. , Maaroufi, A. and Isaert, N.(1992) 'New TGB_A series exhibiting a S_C*$S_A$$S_A$*N* phase sequence', Liquid Crystals, 12: 4, 575 — 591
To link to this Article: DOI: 10.1080/02678299208029094
URL: http://dx.doi.org/10.1080/02678299208029094

LIQUID CRYSTALS, 1992, VOL. 12, NO. 4, 575–591

New TGB_A series exhibiting a $S_C^*S_AS_A^*N^*$ phase sequence

by A. BOUCHTA†, H. T. NGUYEN*, M. F. ACHARD,
F. HARDOUIN, C. DESTRADE
Centre de Recherche Paul Pascal, Avenue A. Schweitzer,
F33600 Pessac Cedex, France

R. J. TWIEG
IBM Almaden Research Center, 650 Harry Road,
San Jose, California 95120-6099, U.S.A.

A. MAAROUFI
Université de Tetouan, Département de Chimie, BP 5204,
Tetouan, Morocco

and N. ISAERT
Laboratoire de Dynamique et Structure des Matériaux Moléculaires,
(U.R.A, CNRS No. 801), Université de Lille 1, U.F.R. de Physique,
F59655 Villeneuve d'Ascq Cedex, France

(*Received 2 January 1992; accepted 27 March 1992*)

A new series with a chiral tolane core has been synthesized. These materials belong to the optically active series: 3-fluoro-4-[(*R*) or (*S*)-1-methylheptyloxy]4′-(4″-alkyloxy-3″-fluorobenzoyloxy)tolanes (*n*FBTFO$_1$M$_7$). For the first time, the helical S_A^* phase or TGB_A phase is found in all of the derivatives from heptyloxy to octadecyloxy. The S_A–S_A^*–N* phase sequence is observed in several compounds with short chains and the S_C^*–S_A–S_A^*–N* phase sequence is obtained with the decyloxy derivative. The TGB_A phase has filament or cholesteric textures. The helical pitch of the TGB_A phase is short for the octadecyloxy derivative and is compared with that for different chain lengths as a function of temperature. The layer spacing in the TGB_A phase shows that it is incommensurate with the fully elongated molecular length.

1. Introduction

Since the discovery of the new helical smectic A phase (TGB_A) by Goodby *et al.* [1, 2] in 1989, the search for such new types of materials has accelerated together with structural [3] and theoretical [4–6] studies as well as the identifying phase sequences [7–10]. These results are consistent with a structure where the molecules are packed in layers and the blocks of the S_A^* rotate around the direction normal to the molecular long axes and parallel to the layers in forming a helical structure [3]. This phase has been found in three different series:

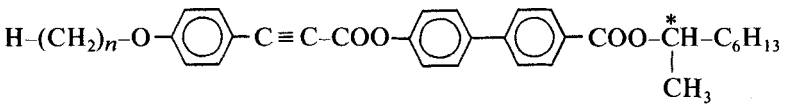

(I)

* Author for correspondence.
† Permanent address: Université de Tetouan, Département de Chimie, BP 5204, Tetouan, Morocco.

0267–8292/92 $3·00

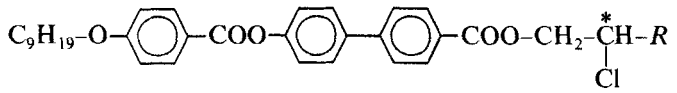

(II)

and

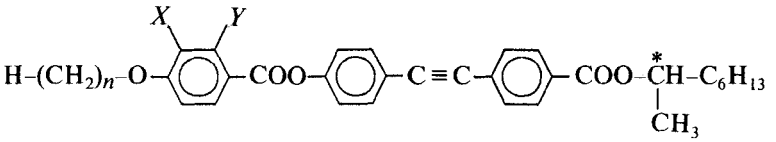

(III)

where

$$R = -CH_3, -CH_2-\underset{\displaystyle CH_3}{\underset{|}{CH}}-CH_3$$

and $X, Y = H, F$. If in series I [1, 2] and III [10], the helical S_A^* phase with the sequence C S_C^* S_A^* I is obtained with very long alkyloxy chains, then the pure compounds of series II display the new sequence $CS_AS_A^*N^*BP$ I. In these three series the chiral chains are attached to the core by the group –COO– which favours the formation of the S_A phase.

In this study, we also explore the influence of the tolane core (as series III) but we replace the ester link for a terminal group attached to the core by an ether link. The new series has the general formula (nFBTFO$_1$M$_7$):

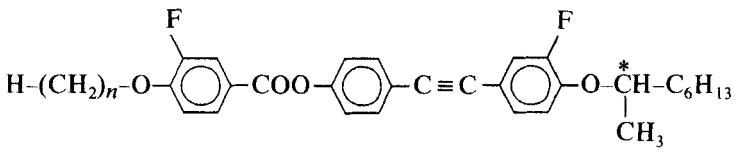

(IV)

where $n = 7$–18.

2. Results and discussion

2.1. *Synthesis*

The compounds of series (IV) were prepared following the scheme:

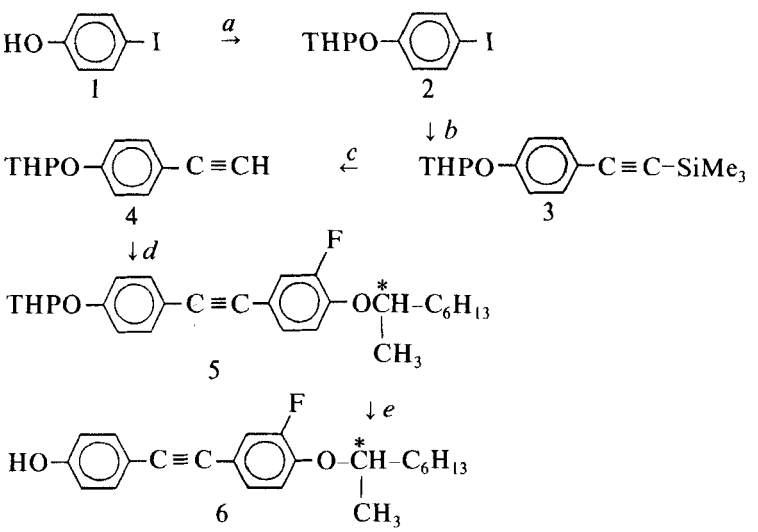

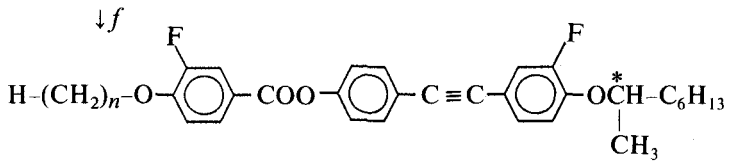

(*a*) DHP,PTSA,CH_2Cl_2,
(*b*) $HC\equiv CSiMe_3$,$PdCl_2$,$Cu(OAc)_2.H_2O$,Ph_3P,iPr_2NH,
(*c*) NaOH 50 per cent, MeOH,THF

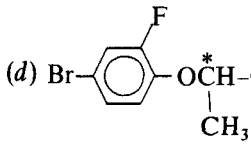

(*d*) $PdCl_2$, $Cu(OAc)_2.H_2O$, Ph_3P, iPr_2 NH,

(*e*) PTSA,THF,MeOH,

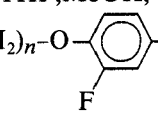

(*f*) COOH (8), DCC, DMAP, CH_2Cl_2

The synthesis details of these new compounds are given in the Experimental.

Transition temperatures (°C) and enthalpies in italic (kJ mol^{-1}) of compounds *n*FBTFO$_1$M$_7$.

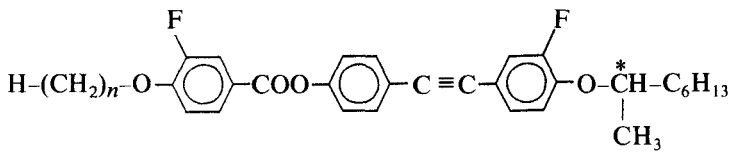

n	C		S_C^*		S_A		S_A^*		N*		BP		I
7	●	59·0 *20·2*	—		●	99·4	●	100·1 *1·00‡*	●	108·6	●	108·6 *0·86†*	●
8	●	64·0 *23·4*	—		●	105·0	●	105·7	●	110·2 *1·30*	●	110·4 *1·00†*	●
9	●	59·4 *26·2*	—		●	100·8	●	101·8 *0·79*	●	106·1	●	106·3 *1·03†*	●
10	●	63·4 *23·1*	●	92·8	●	101·2	●	102·6 *0·86‡*	●	105·2	●	105·4 *1·12†*	●
11	●	68·0 *21·1*	●	97·4 *0·27*	—		●	100·5 *0·29*	●	103·5	●	103·7 *3·16†*	●
12	●	69·0 *23·6*	●	97·6 *0·15*	—		●	99·9 *0·12*	●	102·7	●	103·7 *3·10†*	●
13	●	67·0 *22·2*	●	97 *0·26*	—		●	98 *~0*	●	101·2	●	101·3 *2·64†*	●
14	●	63·6 *20·2*	●	98·2 *0·7*	—		●	98·8 *~0*	●	101	●	101·2 *2·63†*	●
16	●	61·0 *55·4*	●	98 *0·67*	—		●	99·3	●	99·8 *5·62§*	—		●
18	●	66·0 *65·0*	●	97·3	—		●	98 *6·28§*	—		—		●

† The sum of two or three transitions: BP–I and N*–BP.
‡ The sum of two transitions: N*–S_A^* and S_A^*–S_A.
§ The sum of two transitions: I–N* and N*–S_A^* or I–S_A^* and S_A^* and S_C^*.

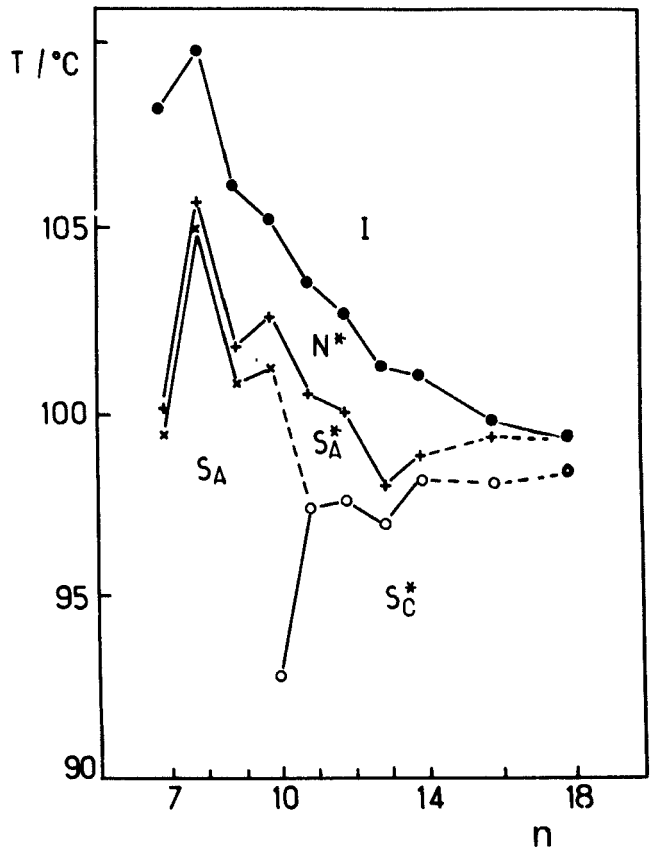

Figure 1. Plots of transition temperatures versus n, the number of carbon atoms in the terminal chain.

2.2. *Mesomorphic properties*

All of the compounds (IV) are mesogenic. The phase assignments and corresponding transition temperatures were determined both by thermal microscopy (Mettler FP 5) and by differential scanning calorimetry (Perkin–Elmer DSC7). The liquid crystal transition temperatures and enthalpies for these new materials are presented in the table and figure 1.

2.2.1. *Microscopic observations*

From the table, it can be seen that the first three members of the series (from heptyloxy to nonyloxy) do not exhibit the S_C^* phase which only makes its appearance from $n=10$. The classic S_A phase is observed from $n=7$ to $n=10$ with focal-conic or homeotropic textures. Most of the compounds display a cholesteric phase and two or three blue phases; the TGB_A or S_A^* phase is obtained in all members of the series. For example, the decyloxy derivative $10FBTFO_1M_7$ was found to have the following phases and transition temperatures:

C 63·4°C S_C^* 92·8°C S_A 101·2°C S_A^* 102·6°C N* 105·2°C BP_I 106·1°C BP_{II} 106·8°C I.

On cooling the compound from the isotropic phase between two glass plates, we observed blue phase II and blue phase I with an iridescent platelet defect texture but the

blue phase III was very difficult to detect. On further cooling from the blue phase I, the cholesteric phase appeared with a focal conic or Grandjean plane texture (see figure 2 (*a*)). On further slow cooling, the transition S_A^*–N* occurred and the helical S_A^* phase was characterized by another Grandjean plane texture (see figure 2 *b*)). When the helical S_A^* transformed into an S_A phase, we observed several dechiralization lines at the transition and then in the S_A phase, classic focal-conic or homeotropic texture (see figure 2 (*c*)). At lower temperatures, the ferroelectric S_C^* phase appeared both with broken fan shaped and plane textures (see figure 2 (*d*)). From undecyloxy to hexadecyloxy derivatives the S_A phase disappeared and a direct S_C^*–S_A^* transition was obtained and for the first time the S_C^* S_A^* N* sequence. In this case, on cooling from the helical S_A^* phase, this transition occurred with the appearance of dechiralization lines (see figure 3) which disappeared to give a classical chiral S_C^* phase. The octadecyloxy member of the series displays the sequence C S_C^* S_A^* I already observed in four series I [1] and III [10] and the helical S_A^* phase is definitely characterized with this compound and others by different complementary techniques: DSC, racemic mixtures, the contact method, X-ray diffraction and pitch measurement.

2.2.2. *Calorimetric studies*

Transition enthalpies were determined by differential scanning calorimetry using a Perkin–Elmer DSC7 and are given in the table. Generally the enthalpy values for the S_C^*–S_A^* or S_C^*–S_A transitions were too small to be measured but when it is possible they range between 0·1 to 0·7. The S_C^*–S_A^* transition enthalpies increase with the chain length. We must point out that as the S_A–S_A^* and S_A^*–N* transitions or N*–BP and BP–I transitions are very close, it is very difficult to obtain separate transition enthalpies and we give the sum of these transition enthalpies. The melting enthalpies ranged between 20 to 26 kJ mol^{-1} except for two very long chains ($n = 16$ and 18) when they are around 60 kJ mol^{-1}.

Now the most striking result obtained from calorimetric studies concerns the S_A–S_A^* and S_A^*–N* transitions. Let us point out that the new S_A–S_A^*–N* phase sequence was first reported in a mixture by Lavrentovich *et al.* [7] and then in a pure compound by Slaney *et al.* [8, 9]. In our series, the S_A–S_A^* transition is observed in four pure members ($n = 7$–10). Typical thermograms are shown in figures 4 (*a*)–(*f*) for heating rates of 0·5°C min^{-1}. In this figure only the transitions near the clearing points are given and they are identical to those shown by Slaney *et al.* (see figure 6 of [8]). Figure 4 (*a*) shows five peaks over a 10°C temperature range, they correspond to different phase transitions: S_A to S_A^*, S_A^* to N*, N* to BP_I, BP_I to BP_{II} and BP_{II} to I. The sum of the three last high temperature transition enthalpies (N* to BP_I, BP_I to BP_{II} and BP_{II} to I) do not change with the chain length but that of S_A to S_A^* and S_A^* to N* decrease with the chain length (except for the heptyloxy member of the series). This fact shows that the former appeared to be first order but the latter must be second order for the long chains. For the short chains the two S_A^*–N* and S_A–S_A^* transitions cannot be separated and we cannot evaluate the first or second order character of these transitions. For example, the S_A^*–N* transition enthalpies are too weak, about 0·29 kJ mol^{-1} and 0·12 kJ mol^{-1} for $n = 11$ and $n = 12$, respectively and almost zero for longer chains (figure 4 (*e*) and (*f*)). The thermograms for cooling rates of 0·5°C min^{-1} showed the same results but there was a slight depression in transition temperature due to supercooling of the blue phases.

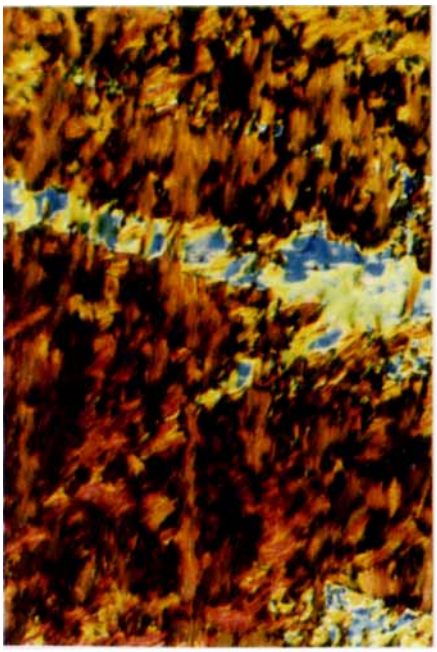

(*b*)

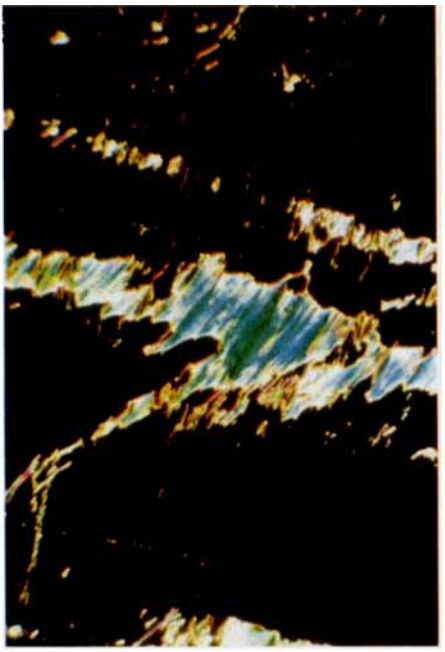

(*d*)

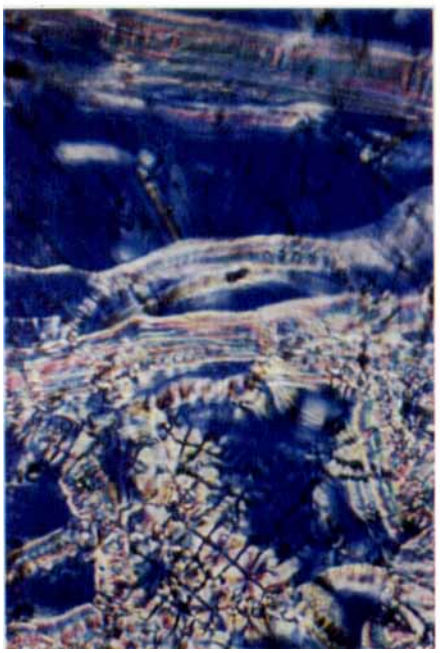

(*a*)

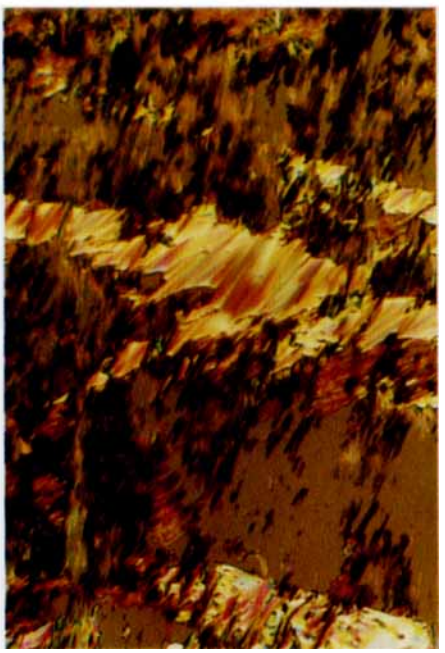

(*c*)

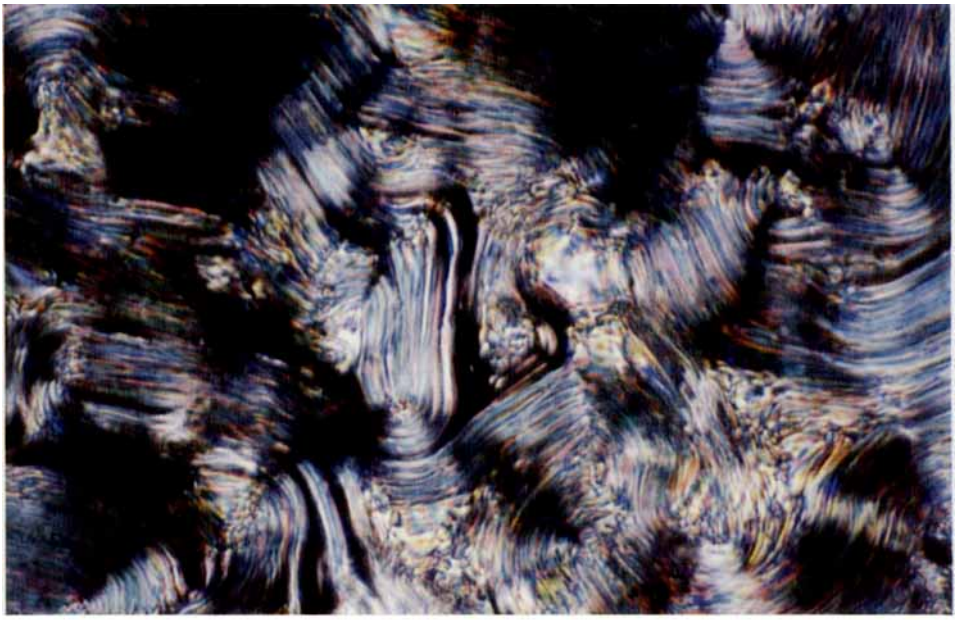

Figure 3. Optical texture of the transition from S_A^* to S_C^*.

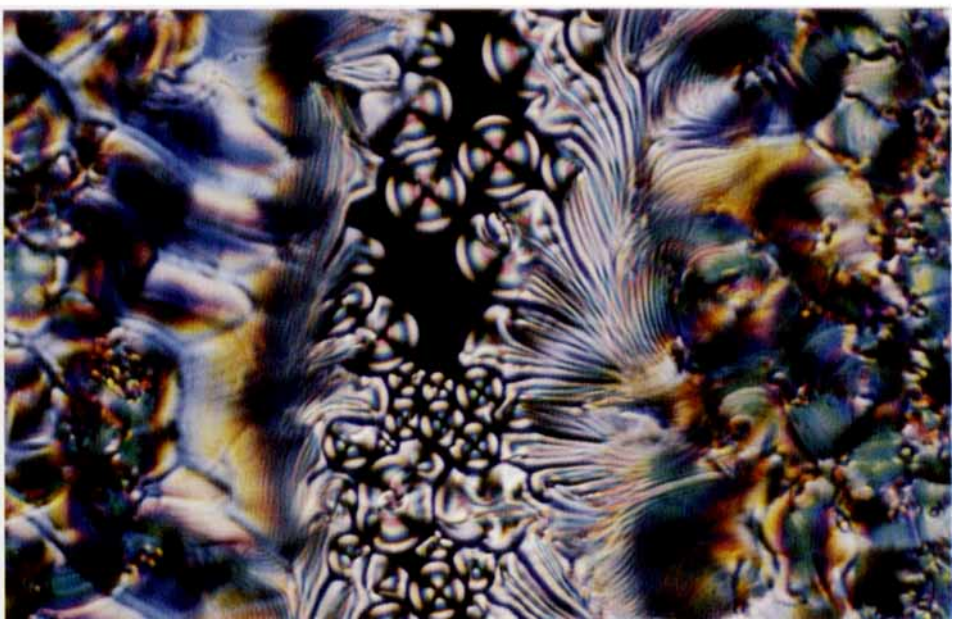

Figure 5. Contact preparation between (*R*) and (*S*) 18FBTFO$_1$M$_7$ enantiomers.

Figure 2. Optical textures of different mesophases of (*R*)-10FBTFO$_1$M$_7$. (*a*) N* phase at 103°C; (*b*) S_A^* phase at 102°C; (*c*) S_A phase at 100°C; (*d*) S_C^* phase at 95°C.

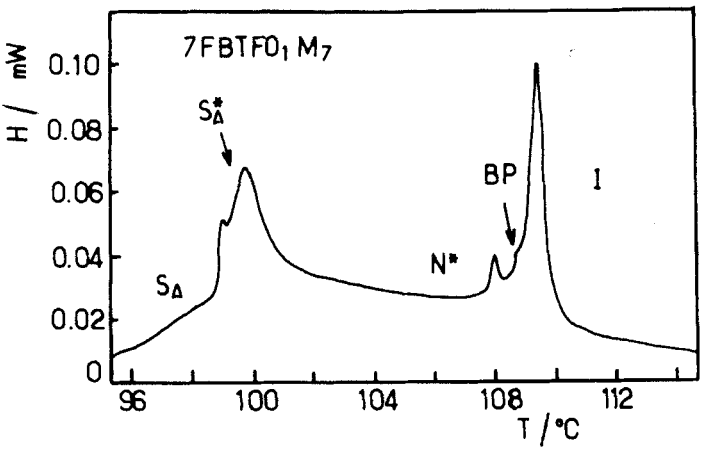

(*a*)

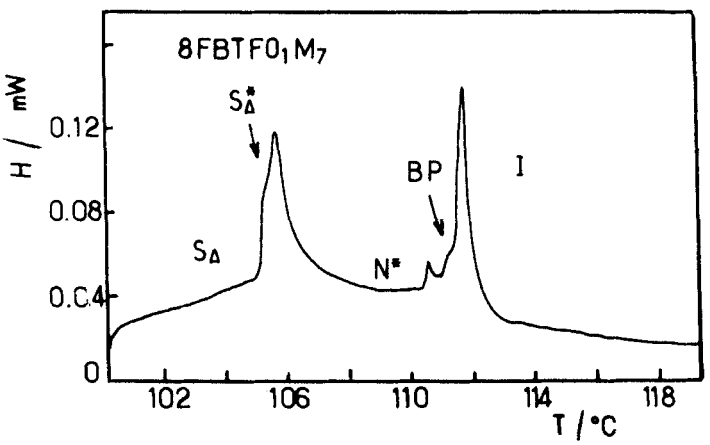

(*b*)

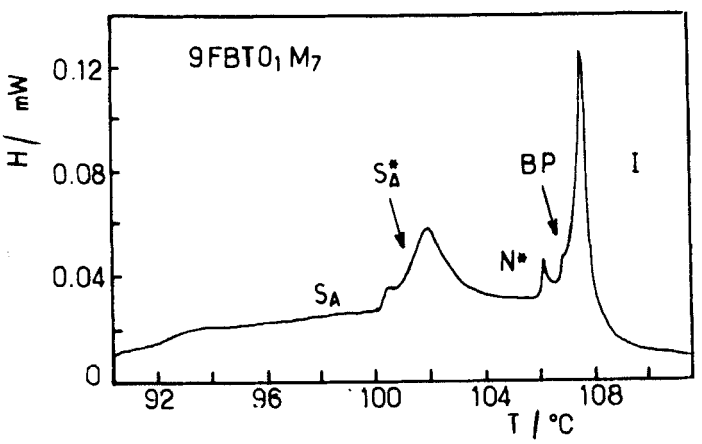

(*c*)

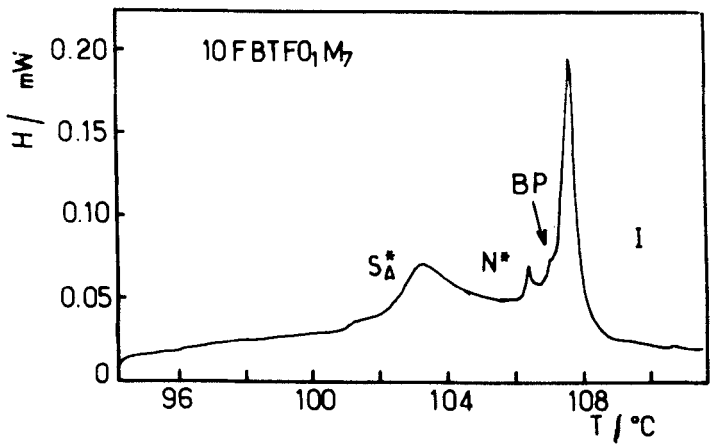

(*d*)

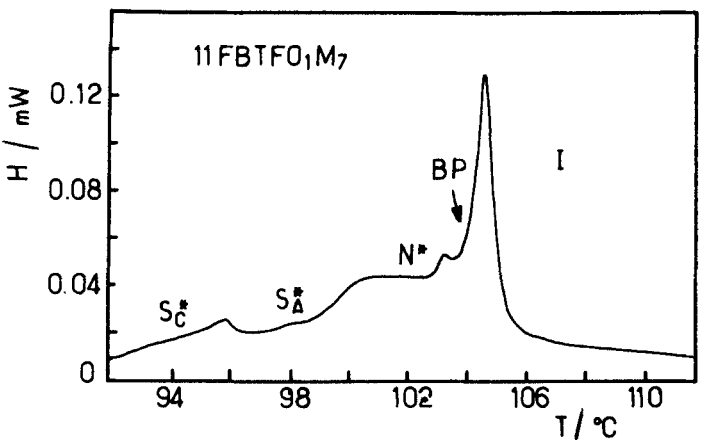

(*e*)

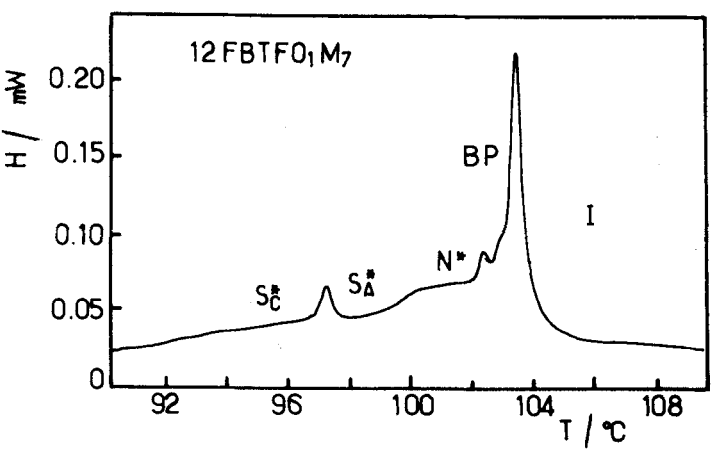

(*f*)

Figure 4. Differential scanning calorimetry thermograms for the heating cycle of nFBTFO$_1$M$_7$. Heating rate = 0·5°C mn^{-1}. (*a*) $n=7$; (*b*) $n=8$; (*c*) $n=9$; (*d*) $n=10$; (*e*) $n=11$; (*f*) $n=12$.

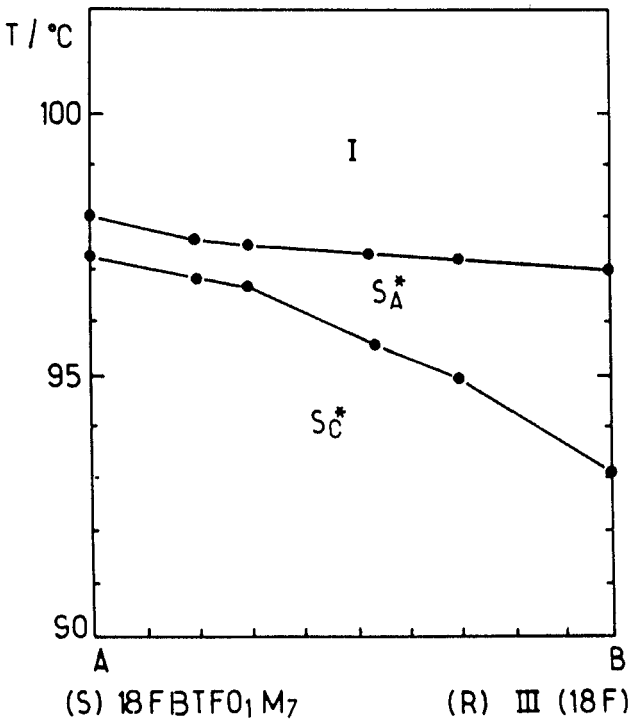

Figure 6. The miscibility phase diagram of binary mixtures between (*S*)-18FBTFO$_1$M$_7$ (on left) and (*R*)-III (18F) (on right).

2.2.3. *TGB$_A$ of 18FBTFO$_1$M$_7$*

The existence of the TGB$_A$ or helical S_A^* phase in this series *n*FBTFO$_1$M$_7$ is at first proved with the octadecyloxy derivative which displays two mesophases: the phase at low temperature is the ferroelectric S_C^* phase and the high temperature one has a Grandjean plane texture similar to a cholesteric. The latter is definitely not a cholesteric phase for the following reasons.

(i) The racemic 18FBTFO$_1$M$_7$ compound exhibits the following phase sequence: C 57°C S_C 97°C S_A 103°C I.

(ii) The contact method between two enantiomers (*R*) and (*S*) of 18FBTFO$_1$M$_7$ (see figure 5) shows in the middle of the preparation, corresponding to the racemic mixture, a S_A phase with focal conic or homeotropic textures. Moving away from the middle we can see a helical S_A^* phase with filament texture and then a S_A^* phase with cholesteric texture corresponding to the pure (*R*) and (*S*) enantiomers.

(iii) We have studied the phase miscibility between (*S*)-18FBTFO$_1$M$_7$ and (*R*)-18F of series III with the formula and phase sequence [10]:

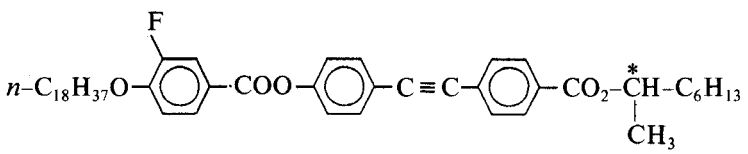

C67°C S_C^* 93°C S_A^* 97°C I.

The helical S_A^* pitch measurement of the last compound showed that the helix sense is right-handed [10]. In this study, the miscibility of the S_C^* and S_A^* phases of these materials is complete and the corresponding phase diagram (figure 6) shows thermodynamic ideality. This is the first example of the miscibility between the S_A^* phases of two different series. It also showed that the helix sense of the S_A^* phase of the (*S*)-18FBTFO$_1$M$_7$ is right-handed.

(iv) Concerning the structural study, X-ray scattering was performed for a powder and an unaligned sample with a high temperature Guinier Camera using monochromatic Co K_{α_1} radiation. In figure 7, we can see that, upon heating the layer spacing of the ferroelectric S_C^* phase is constant ($d_{S_C^*} = 41{\cdot}5$ Å) and near the S_C^*–S_A^* transition, it increases and saturates in the S_A^* phase ($d_{S_A^*} = 43{\cdot}9$ Å). It is clear that the layer spacing $d_{S_A^*}$ of this compound is not commensurate with the fully extended molecular length ($l = 55$ Å) and is more than 11 Å lower. This behaviour is often observed with very long alkyloxy chains which have a folded shape in order to fill space. With $d_{S_A^*}$ and $d_{S_C^*}$ we calculate the highest tilt angle θ in the S_C^* phase from $\cos\theta = d_{S_C^*}/d_{S_A^*}$ which gives $\theta = 19°$. This angle is often smaller to that obtained from the electrooptical measurements. We give more details in the next paragraph.

(v) The helical character of this S_A^* phase is demonstrated by the pitch measurement. The helical twist is studied on prismatic samples using very clean rubbed glasses forming a small angle (0·25°). Excellent planar orientations can be obtained, with regular Grandjean–Cano steps allowing helical pitch measurements. The rotatory power can also be studied; its sign gives the helix sense.

The pitch of the (*R*)-18FBTFO$_1$M$_7$ compound was measured over the whole S_A^* phase temperature range (≈0·6°C). The pitch varies from 0·40 μm to 0·47 μm, and produces red coloured light selective reflection. The pitch of four compounds are compared in figure 8 ($n = 18, 16, 11, 7$): for $n = 16$, its value varies from 0·5 to 0·4 μm in the S_A^* phase, and decreases down to 0·28 μm in the N* phase, producing blue selective reflection. For $n = 11$, the pitch in the N* phase is only 0·2 μm near the isotropic phase with ultraviolet selective reflection. It increases regularly, without any divergence, in the S_A^* phase, up to about 3 μm near the S_C^* phase. For $n = 7$, the behaviour is quite different. The pitch is very

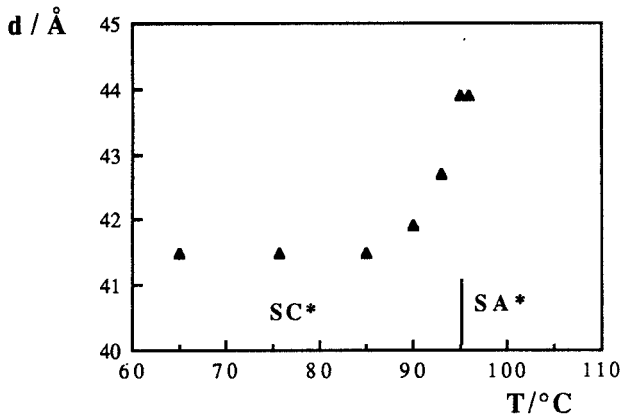

Figure 7. The temperature dependence of the layer spacing for (*S*)-18FBTFO$_1$M$_7$.

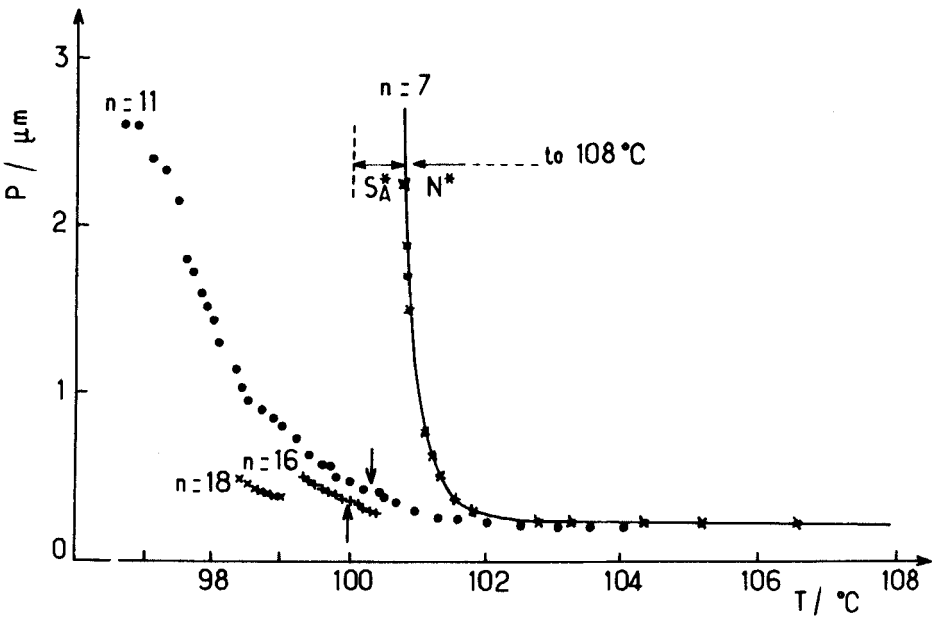

Figure 8. Helical pitch variations in the S_A^* phase of (*R*)-18FBTFO$_1$M$_7$; in the S_A^* and N* phases of (*R*)-16 and (*R*)-11FBTFO$_1$M$_7$ (arrows give the approximate S_A^*–N* transition temperature); in the N* phase of (*R*)-7FBTFO$_1$M$_7$.

small in almost the whole N* phase, starting from 0·2 µm at high temperature, but it suddenly presents a noteworthy pretransitional divergence at the S_A^* phase, this divergence being due to the proximity of a S_A phase. This divergence is not complete and it is possible to observe the twisted S_A^* phase over about 0·6°C, with a pitch varying from about 3 µm to 10 µm. The pitch measurements are then inaccurate and are not given in figure 8. All these (*R*) compounds show a left rotatory power for wavelengths lower than the selective reflection band and the helix sense is then left handed.

These results show unambiguously that the high temperature mesophase of the 18FBTFO$_1$M$_7$ is a helical S_A^* phase. The 50:50 weight mixtures between $n=18$ and $n=16$, $n=16$ and $n=14$, $n=14$ and $n=12$, $n=12$ and $n=10$ proved the miscibility of the TGB_A phases in these compounds as given in figure 1.

2.3. *Electrooptical properties*

We have studied the electrooptical properties of these compounds in the surface stabilized ferroelectric liquid crystal configuration, including the temperature dependence of the response time, polarization and tilt angle. The device used for the ferroelectric measurements is reported in an earlier paper [11]. The sample thickness is around 3 µm (checked by the Newton fringe method). The recurrence frequency is 3 kHz and the applied field corresponding to saturation is around 30 V. Figure 9 shows relatively high polarization of about 65 and 60 nC cm^{-2}, respectively, for the tetradecyloxy and octadecyloxy derivatives. The response time of these new materials is fairly fast, below 25 µs at 70°C for two longer chains and about 10 µs for the decyloxy derivative under a field of 10 V µm^{-1} (see figure 10). It is interesting to note that near the

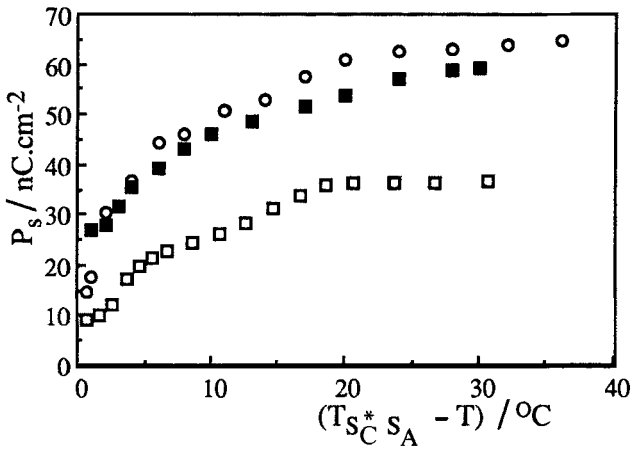

Figure 9. Spontaneous polarization versus $T_{S_C^*S_A} - T$. □ $n=10$, ○ $n=14$, ■ $n=18$.

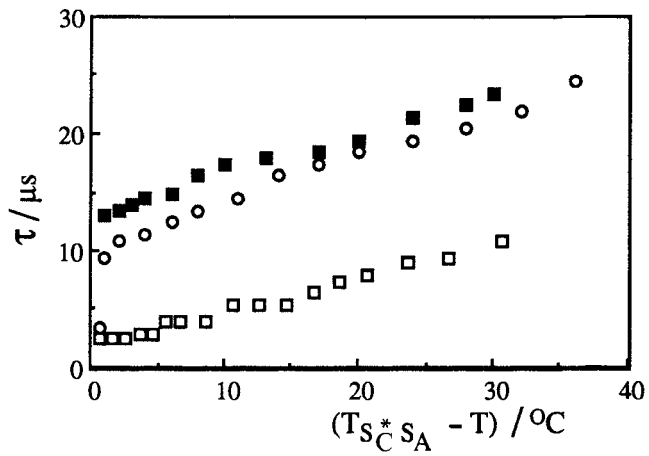

Figure 10. Response time versus $T - T_{S_C^*S_A}$ ($N=3$ kHz, $E=5$ V μm^{-1}).

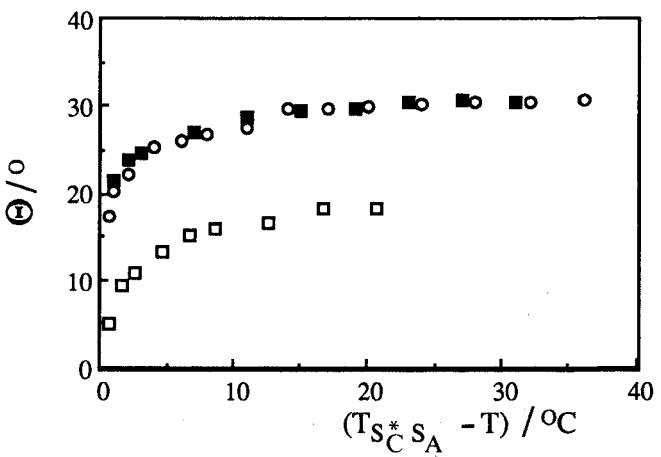

Figure 11. Tilt angle versus $T_C^*S_A - T$. □ $n=10$, ○ $n=14$, ■ $n=18$.

S_C^*–S_A or S_C^*–S_A^* transition, the optical tilt angle variation is different following the S_C^*–S_A or S_C^*–S_A^* transition. With $n=10$ and the S_C^*–S_A transition, the tilt angle starts with a low value ($\sim 5°$) but for the S_C^*–S_A^* transition, this angle is very high, near 20° (see figure 11). The behaviour of the helical S_A^* phase is intermediate between the N* and S_A phases because near the S_C^*–N* transition (without a virtual S_A phase), the tilt angle is very high, about 30°, and saturates at a value close to 45° while it was found to saturate at 31° for $18FBTFO_1M_7$. This value is higher than that calculated from the layer spacings $d_{S_C^*}$ and $d_{S_A^*}$ (19°). This tends to suggest the use of a surfactant for alignment in electrooptical measurement favours the pretilt in the S_A^* phase and in the S_C^* phase the tilt angle is higher.

2.4. *Discussion*

The helical S_A^* phase was predicted first by de Gennes [4] in 1972 comparing the S_A–N* transition and the metal normal-superconductor transition in an external magnetic field. Then Renn and Lubensky [5,6] in 1988 described this phase as a frustrated intermediate between N* and S_A phases but it was first demonstrated in pure materials [1,2] with the sequence C S_C^* S_A^* I. The exact predicted sequence C S_A^* S_A N* I was first obtained in a mixture [7] and then in a pure compound [8,9] which was identified by thermal and optical studies. It has also been found in polymeric systems [12–14]. In this new series nFBTFO$_1$M$_7$, the optical, thermal, structural, mixture and pitch measurement results indicate clearly that the compound $18FBTFO_1M_7$ displays the same sequence C S_C^* S_A^* I as observed in the Goodby series [1] and in ours [10]. The mixtures studied between this compound and others with short chains together with optical and thermal results show that the TGB_A also exist either between N* and S_A phases or N* and S_C^* phases. So we can assess the helical S_A^* phase in the short chain derivatives with the help of thermal diagrams identical to that of Slaney *et al.* [8,9] and also to the complete series. The existence of the helical S_A^* phase depends mainly on the molecular polarity, especially the polarity near the chiral centre and, of course, on the chiral chains and the optical purity. As a matter of fact, when Slaney *et al.* [8,9] replaced the chiral 2-octanol chain by chiral primary alcohols derived from amino acids, they obtained a new sequence with the S_A^* phase between S_A and N* phases. Now if the link group between the chiral chain and the core is replaced, for example, the –COO– group by –O–, the S_A phase is disfavoured to the cholesteric and in this case, we could not observe the S_A^* phase. This tends to suggest that the S_A phase is favoured by the transverse polarity of the linking group. Now, for increasing the transverse polarity of the –O– link group, an electronegative substituent fluorine, for example, is introduced in the *ortho* position, it prefers to take the following position [16]:

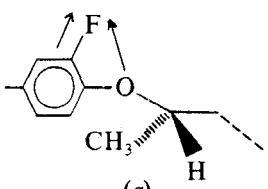

(*a*)

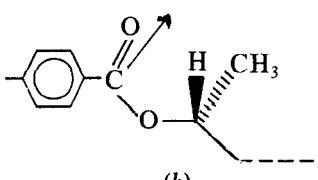

(*b*)

Now the transverse polarity of (*a*) is comparable to that of (*b*) and the S_A phase is observed in all series. But if the fluorine is replaced by a CN group which favours S_A phase formation the helical S_A^* phase could not be observed.

3. Experimental

The infrared spectra were recorded using a Perkin–Elmer 783 spectrophotometer and the NMR spectra with a Bruker 270 MHz. All final compounds give satisfactory elemental analyses.

3.1. *1-Iodo-4-tetrahydropyranyloxybenzene* (**2**)

To a stirred solution of 4-iodophenol (150 g; 72·72 mmol) in CH_2Cl_2 (400 ml), cooled in an ice bath, dihydropyran (72·3 g; 87·7 mmol) was added dropwise over 10 min. The solution became clear, and some crystals of *p*-toluenesulphonic acid (PTSA) were then added. The reaction started and was complete after 15 min (TLC) shows no starting material remaining). The reaction was quenched by addition of $NaHCO_3$ (4 g). The solvent was removed by rotary evaporation and the solid was dissolved in EtOAc and filtered through silica gel. The solvent was removed and the residue recrystallized from hexane in a plastic bottle. Yield: 195 g (95 per cent), mp = 65°C. 1 H NMR ($CDCl_3$, δ): 1·6–2 (m, 6H of THP), 3·5 (m, 1 H, THP), 3·9 (m, 1 H, THP), 5·4(T, 1 H of O–CH–O), 6·8–7·6 (2d, $J = 8$ Hz, 4 H arom.). IR (Nujol): 1630, 1620, 1280, 1160, 1110, 970, 870 cm^{-1}.

3.2. (*4-Tetrahydropyranyloxy*)*phenylacetylene* (**4**)

A solution of **2** (66 g; 0·217 mol), triphenylphosphine (TPP) (1·44 g; 5·5 mmol) in diisopropylamine (200 ml) was heated at 30°C under nitrogen. To this clear solution, were added catalysts $PdCl_2$ (200 mg; 1·1 mmol) and $Cu(AcO)_2$ H_2O (200 mg; 1 mmol). The solution was degassed, then TMS acetylene (25 g; 0·255 mol) was added dropwise to the solution which was gradually heated with an oil bath (80°) for 2 h. A salt formed and after 2 h the solution was cooled to room temperature, filtered off and washed well with hexane. The filtrate was evaporated to dryness and hydrolysed with concentrated hydrochloric acid (10 ml) and crushed ice (50 g). Organic materials were extracted with hexane (2 × 300 ml) and the organic phase washed with water (250 ml), dried over Na_2SO_4, filtered and evaporated. The residue was filtered on silica gel with (9 : 1) hexane ethyl acetate mixture. The solvent was removed on a rotary evaporator and the compound **3** (47 g) was dissolved in THF (70 ml) and methanol (70 ml). To the solution cooled in an ice bath was added dropwise with stirring a 50 per cent NaOH solution (16 g). The solution was stirred at room temperature for 1 h. It was brought up to 1 l with hexane (400 ml) and water (400 ml). The organic phase was washed once with 300 ml of water, dried over anhydrous Na_2SO_4, filtered and evaporated. The compound **4** was filtered through silica gel and recrystallized from hexane. Yield: 30·1 g (69·6 per cent) mp = 65·5°C. 1 H NMR($CDCL_3$, δ): 1·6–2·1 (m, 6H of THP), 3·0 (s, 1 H, C≡CH), 3·6 (m, 1 H, THP), 3·9 (m, 1 H, THP), 5·4 (*t*, 1 H, O–CH–O), 6·9–7·5 (2 d, $J = 8$ Hz, 4 H arom.). IR (Nujol): 3280, 1600, 1280, 1170, 1110, 970, 840 cm^{-1}.

3.3. (*R*)-*1-Bromo-3-fluoro-4-*(*1-methylheptyloxy*)*benzene* 7

To a cooled solution of 4-bromo-2-fluorophenol (8·5 g; 44·6 mmol), (*S*)-2-octanol (5·8 g; 44·6 mmol), TPP (12·5 g; 47 mmol) in CH_2Cl_2 (100 ml) was added dropwise diethylazodicarboxylate (8·5 g; 48·8 mmol) [17]. The solution was stirred at room temperature for 3 h. The solution was filtered, evaporated and chromatographed on

silica gel with (95 : 5) hexane ethyl acetate mixture. Yield: 10·3 g (72 per cent). 1 H NMR ($CDCl_3$, δ): 0·89 (t, 3 H, CH_3 of C_6H_{13}, 1·3 (m, 6 H, $3CH_2$), 1·37 (d, 3 H of CH_3–CH), 1·6–1·8 (m, 2 H, OCH–CH_2–), 4·3 (m, 1 H, CH–CH_3), 6·9 (t, 1 H arom. *ortho* to OR), 7·5 (d, $J = 8$ Hz, 2 H arom. *ortho* to Br). IR (Nujol): 1610, 1280, 1170, 1120, 960 cm^{-1}.

3.4. *(R)-3-Fluoro-4-(1-methylheptyloxy)-4'-hydroxytolane* **6**

In a 250 ml round bottomed flask were placed **4** (8 g; 0·04 mol), **7** (13.3 g; 0·044 mol), TPP (1 g; 3·8 mmol) in dipropylamine (120 ml) under nitrogen. The solution was stirred and heated in an oil bath at 30°C until complete dissolution. Then catalysts $PdCl_2$ (110 mg; 0·6 mmol) and $Cu(AcO)_2$; H_2O (120 mg; 0·6 mmol) were added to this solution which was gradually heated to 100°C and maintained at this temperature for 4 h [18]. After cooling to room temperature the salt was removed by filtration and washed well with ethyl acetate. The filtrate was evaporated and hydrolysed with concentrated hydrochloric acid (10 ml), water (100 ml) and crushed ice (50 g) and then extracted with ethyl acetate. The organic phase was dried over anhydrous Na_2SO_4, filtered and evaporated. The residue was filtered on silica gel with (9 : 1) hexane ethyl acetate mixture. The intermediate compound **5** (11 g) was obtained and dissolved in a CH_2Cl_2 (70 ml), CH_3OH (120 ml) mixture. To this solution was added PTSA (0·3 g) and the mixture was stirred at room temperature for 1 h. The solvent was evaporated and the pure phenol **6** was obtained by chromatography on silica gel with (8 : 2) hexane ethyl acetate mixture. Yield: 7·2 g (52 per cent); mp = 39°C. ^{1}H NMR ($CDCl_3$, δ): 0·89 (t, 3 H, CH_3 of C_6H_{13}), 1·29 (m, 6 H, 3 CH_2), 1·35 (d, 3 H of CH_3–CH), 1·6–1·8 (m, 2 H, OCH–CH_2 (s, 1 H, OH), 4·3 (m, 1 H, CH–CH_3), 6·8 (t, 1 H arom. *ortho* to OR), 6·9–7·5 (3d, $J = 8$ Hz, 6 H arom.). IR (Nujol): 3380, 1610, 1260, 1170, 960, 820, 810 cm^{-1}.

3.5. *(R)-3-fluoro-4-(1-methylheptyloxy)-4'-[(4''-decyloxy-3''-fluoro) benzoyloxy]tolane IV* ($n = 10$)

To a solution of phenol **6** (0·7 g; 2 mmol) in CH_2CL_2(5 ml) was added dicyclohexylcarbodiimide (DCC) (0·45 g; 2·2 mmol), 4-dimethylaminopyridine (DMAP) (40 mg) and 3-fluoro-4-decyloxybenzoic acid [11] (0·66 g; 2·2 mmol). The resulting solution was stirred at room temperature overnight. The solution was filtered, evaporated and chromatographed on silica gel with toluene as eluent. The compound was recrystallized from absolute ethanol. Yield: 0·85 g (68 per cent). Transition temperatures: C 63·4°C S_C^* 92·8°C S_A^* 101·2°C S_A 102·6°C N* 105·2°C BP 105·4°C I. 1 H NMR ($CDCl_3$, δ): 0·85 (t, 6 H, $2CH_3$), 1·23 (m-20 H, $10CH_2$), 1·31 (d, 3 H, CH_3–CH), 1·8 (m, 4 H, OCH–CH_2, OCH_2–CH_2), 4·02 (t, 2 H, OCH_2), 4·3 (m, 1 H, CH–CH_3), 6·8 (2t, 2 H arom. *ortho* to OR), 6·9–8·1 (4d, $J = 8$ Hz, 8 arom.). IR (Nujol): 1730, 1610, 1270, 1180, 1120, 960, 850, 820 cm^{-1}.

4. Conclusion

In the new series with the ether link between the core and the chiral chain, the helical S_A^* phase for the highest chain length ($n = 18$) was identified by different techniques. This reference compound is used for miscibility studies of the S_A^* phase in the series and this phase exists now in different phase sequences: C $S_A^*S_A$ N* BP I, C S_C^* S_A^* N* BP I, C S_C^* S_A^* I. A study of the relation between the molecular structure and the existence of TGB_A and TGB_C or TGB_{C*} (also predicted by Renn and Lubensky) is in progress.

The authors wish to thank Drs G. Sigaud and P. Barois for stimulating discussion and their interest in this work.

References

[1] GOODBY, J. W., WAUGH, M. A., STEIN, S. M., CHIN, E., PINDAK, R., and PATEL, J. S., 1989, *Nature*, (*Lond.*), **337**, 449.
[2] GOODBY, J. W., WAUGH, M. A., STEIN, S. M., CHIN, E., PINDAK, R., and PATEL, J. S., 1989, *J. Am. chem. Soc.*, **111**, 8119.
[3] SRAJER, G., PINDAK, R., WAUGH, M. A., GOODBY, J. W., and PATEL, J. S., 1990, *Phys. Rev. Lett.*, **64**, 13.
[4] DE GENNES, P. G., 1972, *Solid St. Commun*, **10**, 753.
[5] RENN, S. R., and LUBENSKY, T. C., 1988, *Phys. Rev.* A, **38**, 2132.
[6] RENN, S. R., and LUBENSKY, T. C., 1991, *Molec. Crystals liq. Crystals*, **209**, 349.
[7] LAVRENTOVICH, O. D., NASTISHIN, Y. A., KULISHOV, V. I., NARKEVICH, Y. S., TOLOCHKO, A. S., and SHIYANOVSKII, S. V., 1990, *Europhysics Lett.*, **13**, 313.
[8] SLANEY, A. J., and GOODBY, J. W., 1991, *J. mat. Chem.*, **1**, 5.
[9] SLANEY, A. J., and GOODBY, J. W., 1991, *Liq. Crystals*, **9**, 849.
[10] NGUYEN, H. T., TWIEG, R. J., NABOR, M. F., ISERT, N., and DESTRADE, C., 1991, *Ferroelectrics*, **121**, 187.
[11] NABOR, M. F., NGUYEN, H. T., DESTRADE, C., MARCEROU, J. P., and TWIEG, R. J., 1991, *Liq. Crystals*, **10**, 785.
[12] FREIDZON, Y. S., TROPSHA, Y. G., TSUKRUK, V., V., SHILOV, V. V., SHIBAEV, V. P., and LIPATOV, Y. S., 1987, *J. Polym. Chem.* (*U.S.S.R.*), **29**, 1371.
[13] BUNNING, T. J., KLEI, H. E., SAMULSKI, E. T., CRANE, R. L., and LINVILLE, R. J., 1991, *Liq. Crystals*, **10**, 445.
[14] GILLI, J. M., and KAMAYE, M., 1992, *Liq. Crystals*, **11**, 569.
[15] KELLY, S. M., 1989, *Helv. chim. Acta*, **72**, 594.
[16] FURUKAWA, K., TERASHIMA, K., ICHIHASKI, M., SAITOH, S., MIYAZAWA, K., and INUKAI, T., 1988, *Ferroelectrics*, **85**, 451.
[17] AUSTIN, W. B., BILOW, N., KELLEGHAN, W. J., and LAU, K. S. Y., 1981, *J. org. Chem.*, **46**, 2280.
[18] MITSUNOBU, O., and EGUCHI, M., 1971, *Bull. chem. Soc. Japan*, **44**, 3427.